

Evolution Of Stoke Vectors And Polarization Measurements In Soft Wood Material Using The Mueller Formalism

*B. Jyothi¹, S. Chandralingam², P. Raghavendra Rao³

¹ Research Scholar, Department of Physics, JNT University Hyderabad.

²Department of Physics, JNTUHCEH, Hyderabad.

³Department of H and S, VNR VJIET, Hyderabad

Corresponding Author: *B. Jyothi

Abstract: A polarimetric apparatus that can measure the optical activity of wood samples was already constructed as part of this research project. The radiation source is a He-Ne LASER that emits at 6328\AA , which falls within the visible spectrum. In this study, we deduced the a whole 4×1 Stokes vector S , which characterises the state of polarisation (SOP) of fully or partially polarised light, as well as the 4×4 Mueller matrix M , which determines the transition of the SOP as light interacts with a material sample. Both of these matrices are necessary for understanding how the SOP changes as a result of light's interaction with the sample. In its most basic form, the Stokes-Mueller calculus is the method that's utilised to illustrate how each instrument functions. It was found that the polarised light was able to pass through the piece of wood, and the degrees of rotation of the polarisation vector of the scattered radiation were figured out. The polarisation of the incident light affects the Stokes parameter, which in turn affects the polarisation parameters that are provided by the Stokes parameter. These include ellipticity, eccentricity, azimuth, and degree of polarisation.

Keywords: Polarization, Stokes parameter, Ellipticity, eccentricity and azimuth.

INTRODUCTION

In recent years, there has been a rise in the demand for more advanced methods of optical characterization that may be used in the processing of materials. This can be due to a variety of different variables, such as the ongoing decrease of components in the semiconductor sector as well as the rapid increase of a diversity of materials in use in optoelectronic devices. Both of these factors are contributing factors in this development. One method for describing the optical properties of a material is to determine its Mueller matrix, which is a mathematical representation of an object's linear optical characteristics along with anisotropy and optical activity [1-2]. Determining a material's Mueller matrix is one way to talk about a material's optical properties. Polarization microscopy is yet another technique that can be utilised. The

Mueller matrix polarimetry (MMP) method has been successfully adopted in order to accomplish this objective by making use of a wide range of experimental approaches [3-13]. The Mueller matrix polarimetry is a common method that offers a feasible strategy for addressing polarisation effects brought on by scattering out from rough surfaces of the a thin film [14-16]. This method is an example of a typical approach. Polarization can be measured with the use of this technique.

According to a thorough interpretation, polarimetric imaging systems can be divided into two basic categories: Mueller matrix polarimeters and Stokes vector polarimeters. A Mueller imaging system contains both a polarisation state generator (PSG) and a polarisation state analyzer (PSA). These components work together to generate totally polarised light and to determine the polarisation state of light which has been dispersed or reflected. This system can provide complete polarised and depolarized information about the data, as well as the capacity to extract the Mueller matrix. In most circumstances, a Stokes vector image system is an excellent solution for a scene that is irradiated by natural light. As a result, it only uses the PSA to determine whether the Stokes vector was reflected or scattered. By adjusting the polarizer, one of the two polarimeters can attain an arbitrarily selected polarisation state. Tyo et al. [17] examine passive Stokes-vector imaging polarimetry for remote sensing applications. Tuchhinn et al. [18] and Gosh and Vithkin [19] discuss active optical polarimetry for biological applications. Optical sensing polarimetry is a method that needs the production and detection of polarisation states. Hauge's [20] provides an excellent review of the apparatus available in the domains of ellipsometry and polarimetry in 1980. Chipman [21] provides the most comprehensive and up-to-date analyses of Mueller matrices and polarimetry.

THEORY

There are four real factors that are referred to as the Stoke parameters, and they can be used to characterise the polarisation state of light. The usual form of this 4-stroke vector is written as a column vector.

$$S = \begin{pmatrix} S_0 \\ S_1 \\ S_2 \\ S_3 \end{pmatrix} \quad \text{----- (1)}$$

Stokes (G.G.Stokes, 1853) discovered the principle of optical correspondence, which indicates that the Stokes vector accurately captures the polarisation phase of a light beam. When interacting with an optical device, scattered light, indicated by such a Stokes vector (S), experiences a linear transformation to create a fresh Stokes vector (S'). This transformation is expressed by the Mueller or Polarization matrix (M), which is a 4 x 4 matrix.

$$S' = M \times S \quad \text{----- (2)}$$

$$\begin{pmatrix} S'_0 \\ S'_1 \\ S'_2 \\ S'_3 \end{pmatrix} = \begin{pmatrix} m_{11} & m_{12} & m_{13} & m_{14} \\ m_{21} & m_{22} & m_{23} & m_{24} \\ m_{31} & m_{32} & m_{33} & m_{34} \\ m_{41} & m_{42} & m_{43} & m_{44} \end{pmatrix} \begin{pmatrix} S_0 \\ S_1 \\ S_2 \\ S_3 \end{pmatrix} \quad \text{----- (3)}$$

Since the Mueller matrix stores all polarisation information, the Stokes vector used to describe the light beam's polarisation is sufficient.

In addition to the standard form, the Mueller matrix M can be represented as

$$M = m_{11} \begin{pmatrix} 1 & \bar{D}^T \\ \bar{P} & m \end{pmatrix} \text{----- (4)}$$

Where $\bar{D}^T = \frac{1}{m_{11}}(m_{12} \quad m_{13} \quad m_{14})$ & $\bar{P} = \frac{1}{m_{11}}(m_{21} \quad m_{31} \quad m_{41})$ called as Diattenuation and Polarization vectors correspondingly and 'm' is a 3 X 3 matrix.

Hans Mueller was the first to employ matrices to perform difficult computations in complex polarisation problems; in fact, the formalism bears the name of as Mueller Matrix formalism. Then calculated the matrices for the rotator, wave plate, and polarizer, which had huge step forward in doing the challenging computations. The Mueller Matrix characterises a polarisation element completely. The Mueller formalism is named after Hans Mueller, who formalised polarisation calculations based on intensity by building arranged the work of Stokes and Perrin.

It is possible that all Mueller Matrices are physically unachievable. The incidence Stokes vector must've been physically realisable from the consequent Stokes vector via the Mueller Matrix for a Mueller Matrix to just be physically realisable. This necessitates also that Degree of Polarization be smaller than or equivalent to one

$$P = \frac{\sqrt{(S_1^2 + S_2^2 + S_3^2)}}{S_0} \leq 1 \quad (5)$$

The inequality [16] is a well-known Mueller Matrix constraint:

$$(MM^T)^T = \sum_{i,j=0}^3 m_{ij}^2 \leq 4m_{11}^2 \quad (6)$$

The diattenuation has been defined as,

$$D = \frac{T_{\max} - T_{\min}}{T_{\max} + T_{\min}} \quad (7)$$

And also values varies from 0 - 1.

As a result, the Mueller Matrix diattenuation is

$$D = \frac{T_{\max} - T_{\min}}{T_{\max} + T_{\min}} = \frac{1}{m_{11}} \sqrt{m_{12}^2 + m_{13}^2 + m_{14}^2} \quad (8)$$

In order to operationally define the diattenuation vector's components, we have

$$D_H = \frac{T_H - T_V}{T_H + T_V} = \frac{m_{12}}{m_{11}}, D_{45} = \frac{T_{45} - T_{135}}{T_{45} + T_{135}} = \frac{m_{13}}{m_{11}} \text{ and } D_C = \frac{T_R - T_L}{T_R + T_L} = \frac{m_{14}}{m_{11}} \quad (9)$$

here T_H denotes transmittance for horizontally polarized light, T_V denotes transmittance for vertically polarized light, T_{45} denotes transmittance aimed at linear 45° polarized light, T_{135} denotes - transmittance for linear 135° polarized light, T_R denotes transmittance for right circularly polarized light and T_L denotes transmittance for left circularly polarized light.

Polarizance is the polarisation that occurs when entirely unpolarized light is converted to polarised light. Polarizance is determined by

$$P = \frac{1}{m_{11}} \sqrt{m_{21}^2 + m_{31}^2 + m_{41}^2} \quad (10)$$

and it take values from 0 to 1.

A description of both the retardance vector as well as the fast axis is given by

$$\bar{R} \equiv R\hat{R} = \begin{pmatrix} Ra_1 \\ Ra_2 \\ Ra_3 \end{pmatrix} \equiv \begin{pmatrix} R_H \\ R_{45} \\ R_C \end{pmatrix} \quad (11)$$

Where the parts represent the horizontal, 45⁰ linear, and circular retardance, respectively. This can be expressed as:

$$R_L = \sqrt{R_H^2 + R_{45}^2} \quad (12)$$

and the whole retardance is

$$R = \sqrt{R_H^2 + R_{45}^2 + R_C^2} = \sqrt{R_L^2 + R_C^2} = |\bar{R}| \quad (13)$$

The formula for the normalised Mueller matrix M is:

$$M = \begin{pmatrix} 1 & m_{12} & m_{13} & m_{14} \\ m_{21} & m_{22} & m_{23} & m_{24} \\ m_{31} & m_{32} & m_{33} & m_{34} \\ m_{41} & m_{42} & m_{43} & m_{44} \end{pmatrix} = \begin{pmatrix} 1 & \bar{D}^T \\ \bar{P} & m \end{pmatrix} \quad (14)$$

Where the sub Matrix m is

$$m = \begin{pmatrix} m_{22} & m_{23} & m_{24} \\ m_{32} & m_{33} & m_{34} \\ m_{42} & m_{43} & m_{44} \end{pmatrix} \quad (15)$$

where \bar{D} & \bar{P} are the diattenuation and polarizance vectors and the diattenuator M_D is considered after the initial row of M, and M_D^{-1} can then be reproduced by M to attain the retarder Matrix $M_R = MM_D^{-1}$. The diattenuator Matrix remains specified by

$$M_D = \begin{pmatrix} 1 & \bar{D}^T \\ \bar{P} & m_D \end{pmatrix} \quad (16)$$

where

$$m_D = aI_3 + b(\bar{D} \cdot \bar{D}^T) \quad (17)$$

Scalars a and b are computed as from norm of the diattenuation vector, with I3 being the identity Matrix for a 3x3 system.

$$D = |\bar{D}|, \quad a = \sqrt{1 - D^2} \quad \text{and} \quad b = \frac{1 - \sqrt{1 - D^2}}{D^2} \quad (18)$$

The Diattenuation vector defines the polarisation element's intensity transmission. When an initial state is unpolarized, the resulting polarisation is described by the Depolarization vector. The concepts of attenuation, depolarization, and retardation are discussed.

The polarisation state of a light beam can be characterised by the Stokes vector denoted by the letter 'S.' The parameter 'S' is defined in relation to the six flux measurements denoted by 'P' that are carried out in front of a radiometer using optimal polarizers. PH horizontal linear polarizer (0°), PV vertical linear polarizer (90°), P₄₅ 45° linear polarizer, P₁₃₅ 135° linear polarizer, PR Right circular polarizer, P_L Left circular polarizer , The definition of the Stokes vector is as follows:

$$S = \begin{bmatrix} S_0 \\ S_1 \\ S_2 \\ S_3 \end{bmatrix} = \begin{bmatrix} P_H + P_V \\ P_H - P_V \\ P_{45} - P_{135} \\ P_R - P_L \end{bmatrix} = \begin{bmatrix} I \\ Q \\ U \\ V \end{bmatrix} \quad (19)$$

where the four elements of the Stokes vector, or Stokes parameters, are S₀, S₁, S₂, and S₃ (or I, Q, U, and V). The resulting polarisation parameters are defined by the Stokes vectors. Flux

$$P = S_0 \quad (20)$$

$$\text{Degree of Polarization DoP} = \frac{\sqrt{S_1^2 + S_2^2 + S_3^2}}{S_0} \quad (21)$$

$$\text{Degree of linear Polarization DoLP} = \frac{\sqrt{S_1^2 + S_2^2}}{S_0} \quad (22)$$

$$\text{Degree of circular Polarization DoCP} = \frac{|S_3|}{S_0} \quad (23)$$

The polarisation ellipse can be described precisely using just four values. The phase at time zero is one of them, while the other three can be any combination of the scale of the semi major axis a, the scale of the semi minor axis b, the alignment of the main axis ψ (azimuth of the ellipse) counter clockwise after the x axis, the eccentricity, and the ellipticity.

$$\text{Ellipticity } \chi = \frac{b}{a} = \frac{S_3}{S_0 + \sqrt{S_1^2 + S_2^2}} \quad (24)$$

$$\text{Major axis orientation (or azimuth)} \psi = \frac{1}{2} \arctan \left(\frac{S_2}{S_1} \right) \quad (25)$$

$$\text{Eccentricity } \varepsilon = \sqrt{1 - \chi^2} \quad (26)$$

EXPERIMENTAL PROCEDURE

A linear polarizer (P) as well as a quarter wave plate were used to provide precise, controlled lighting for the sample (Q1). A second linear analyzer (A) plus quarter wave plate were utilised to determine the polarisation of the light that was captured by the detector after being reflected off of the sample (Q2). While taking measurements, the scattering angle between the Analyzer and the collection optics was kept at 45° degrees from the beam direction. By appropriately rotating the Polarizer and Analyzer, we were able to generate 49 images for the collection of the 4×4 Mueller matrix. A laser with 20m W of power, 632.8 nm of wavelength, and a defined polarisation state was used to illuminate the wood sample. Throughout the experiment, we maintained a 45° angle between the input beam and the collection optics. And this is what we see in Figure 1.



Figure1: Obtaining Mueller matrix elements: an experimental setup diagram

Zingiber officinale is the sample name, and it is a piece of wood that came from a natural source. Chemical analysis (Vitro labs, Hyderabad, India) was performed on the material after it was dried for a year to naturally evaporate the amount of moisture present without causing any changes to the chemical makeup. (Table 1). The average dimensions of the sample are 1.15 millimetres thick, 58.25 millimetres wide, and 136.45 millimetres long after polishing.

Wood sample (Zingiber officinale)					
C %	H %	N %	O %	H ₂ O %	Others %
11.45	46.49	33.18	4.91	2.85	1.12

Table 1: Chemical composition of wood sample

In order for the researchers to determine the intensity of the sample, they started by directing a light source of photons from the source through a PSG towards the sample material. Next, they redirected the beam of photons that was reflected from the sample material through a PSA and onto a CCD detector that was connected to a computer. We captured 49 pictures of differing intensities by adjusting the optical components of the PSG and PSA.

The optical fingerprint of an individual's sample may be located in the Mueller matrix. It is necessary to take 49 images of varying intensities using a variety of polarizer and analyzer directions in order to obtain the 16 components that make up a Mueller matrix image. In order

to obtain the 16-element Muller matrix pictures[18], we first need to acquire 49 intensity images, which are specified as follows.

$m_{11}= I_{OO}$	$m_{21}=I_{OH}-I_{OV}$	$m_{31}=I_{OP} - I_{OM}$	$m_{41}= I_{OL}- I_{OR}$
$m_{12}= I_{HO}-I_{VO}$	$m_{22}=(I_{HH} +I_{VV}) - (I_{HV}+I_{VH})$	$m_{32}=(I_{HP} +I_{VM}) - (I_{HM} +I_{VP})$	$m_{42}=(I_{HL} +I_{VR}) - (I_{HR} +I_{VL})$
$m_{13}= I_{PO}-I_{MO}$	$m_{23}=(I_{PH}+I_{MV}) - (I_{PV}+I_{MH})$	$m_{33}=(I_{PP} +I_{MM})- (I_{PM} +I_{MP})$	$m_{43}=(I_{PL} +I_{MR}) - (I_{PR} +I_{ML})$
$m_{14}= I_{LO}-I_{RO}$	$m_{24}= (I_{RV} +I_{LH}) - (I_{RH}+I_{LV})$	$m_{34}=(I_{RM} +I_{LP}) - (I_{RP} +I_{LM})$	$m_{44}=(I_{RR} +I_{LL}) - (I_{RL} +I_{LR})$

where H denotes horizontal polarisation, V vertical polarisation, and so on for the intensity parameters; the first subscript indicates the input state, and the second subscript the output state P indicates $+45^0$, M indicates -45^0 , Polarization states are denoted by letters, with R representing right circular polarisation and L representing left circular polarisation. Figure 4 displays the equivalent pictures, which were acquired by cropping the image so that each pixel had the same size and using a programme that the author had written in MATLAB to extract information on the image's intensity, one pixel at a time.

After obtaining all 16 photos, they are processed once more with a custom MATLAB software that calculates the intensity component of each pixel in order to acquire the image's data about the scope of the intensity. Because of this transformation, the Muller matrix that was produced as a result has a m11 component, which simplifies the analysis and allows for the separation of intensity-dependent effects from the polarisation effects.

About the sample (Zingiber officinale):

Zingiberaceae is the family name for the ginger family. Originating in Southeast Asia, the majority of today's crop is grown in the Indian states of Andhra Pradesh, Uttar Pradesh, West Bengal, and Maharashtra. Cantonese for "ginger" Ayurvedic: Aardraka, Aadrikaa, Shrngibera, shrngavera, and Katubhadra are all names for its fresh rhizome. Fresh rhizome – Zanjabeel-Ratab, Al-Zanjabeel; dried rhizome — Shunthi, Naagara, Naagaraa, Unani. Zanjabeel rhizome, also known as Zanjabeel-eyaabis, dried up. Siddha's new rhizome varieties include Inji, Allam, and Lokottai. Rhizome chukku, Sunthi's dried version. Rhizome action includes antiemetic, antifatulent, hypocholesterolemic, antiinflammatory, antispasmodic, expectorant, circulatory stimulant, diaphoretic, and enhancing the bioavailability of prescription medications. As a treatment for IBS, diarrhoea, the common cold, and the flu. Interestingly, it worked well in treating both migraines and cluster headaches. Important use: treatment of dyspepsia and avoidance of motion sickness (German Commission E); treatment of nausea and vomiting due to pregnancy, anorexia, bronchitis, and rheumatic symptoms (The British Herbal Compendium); antiemetic use ensuing surgery. (ESCOP). The rhizome produces an vital oil with phenolic ketone derivatives

including gingerols and shogaols, as well as monoterpenes like geranial and neral and sesquiterpenes like beta-sesquiphellandrene, beta-bisabolene, arcurcumene, and alpha-zingiberene. Diarylheptenones, diterpenes, gingesulphonic acid, and monoacyldigalactosyl glycerols are some of the other compounds found here. The digestive enzymes gingerol and shogaol have been found to inhibit stomach acid production. Fresh or dry, rhizomes have the same effect on nausea and vomiting. As a result of its calming, anti-inflammatory, antipyretic, analgesic, hypotensive, and hepatoprotective properties, gingerol and shogaol have recently come into the spotlight.

RESULTS & DISCUSSIONS

Using the aforementioned formulas, we can extract the 16 elemental Mueller matrices from the collected intensity images, which are illustrated in Figure 2 below.

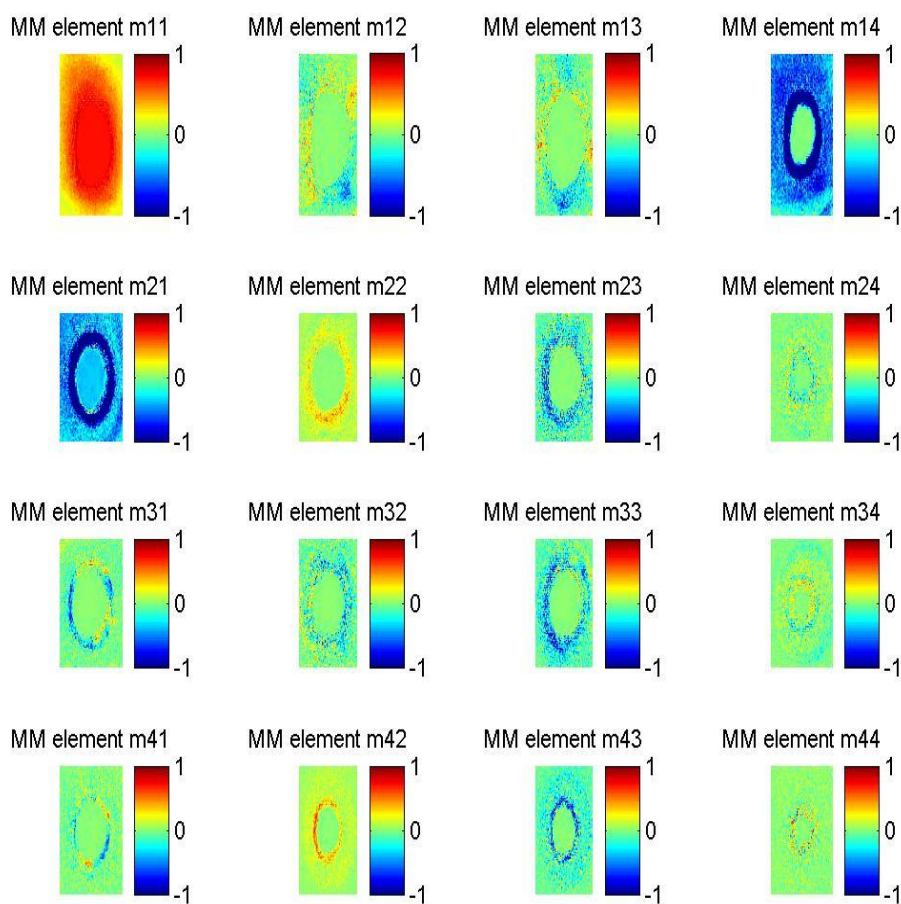


Figure2: pictures of the wood sample in the Mueller Matrix format

After the acquisition of 16 photos, those images are further analysed by means of the MATLAB software in order to get the evaluations of every single pixel contained within the image. This obtained Mueller Matrix is standardized to the initial element of the matrix throughout order to separate the effort effects in the picture and also to facilitate the analysis. Both of these goals were accomplished by focusing on the initial element of the matrix. In the following table, Table 2, you will find a listing of the components that make up the Mueller matrix.

1	0.011989	-0.02936	-0.02734
0.19785	0.16723	-0.08967	-0.01532
0.19898	0.082348	0.071626	0.10672
0.047892	0.31496	0.18349	0.13421

Table 2: Elements of the Mueller matrix contained in the sample

Figure 3 illustrates the pictures of the diattenuation, retardance, & depolarization that were acquired from the measured Mueller matrix. The measured Mueller matrix was used to produce these images. The material's average value both for its attenuation and depolarization can be found in Table 3, which can be accessed by clicking on the respective column headers.

Sample name	Diattenuation	Depolarization	Retardance
Zingiber officinale	0.0123	0.7156	1.9023

Table 3 Values for diattenuation, depolarization, and retardance, on average.

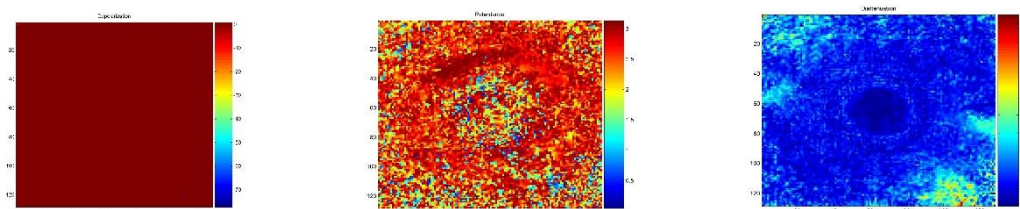


Fig 3: Depolarisation, Retardance and Diattenuation of the wood sample

Stokes vector images S0, S1, S2, and S3 were obtained from these Mueller Matrix pictures after they were processed. However, in order to acquire these photos, images from the Mueller Matrix had to be increased to 512 pixels by 512 pixels, and then they had to be processed pixel by pixel. This was done so that the images would be as clear as possible. Figure.4 displays these newly acquired pictures for your perusal.

The Stokes vector parameters S0, S1, S2, and S3 were derived from all these Stokes vector pictures by utilising a Mat Lab method created specifically for this purpose. They are included in Table 3.

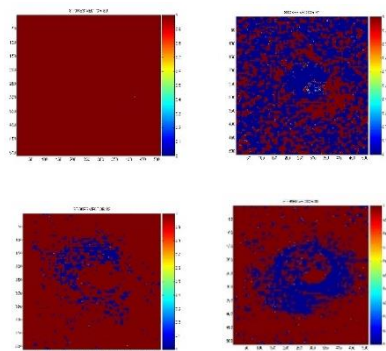


Fig 4. Sample vector images in the Stokes format

Stokes vector average values for Zingiber officinale	
Stokes vector S_0	1
Stokes vector S_1	.3624
Stokes vector S_2	.7545
Stokes vector S_3	.3142

Table 5.3: Stokes vector elemental values for Zingiber officinale

The preceding stokes vector pictures were used to obtain the images of the degree of polarizations (DoP, DoLP, and DoCP), as well as the three polarisation characteristics, namely the ellipticity, eccentricity, and the fast axis orientation azimuth. Figure 5 displays the accompanying pictures that go along with the data..

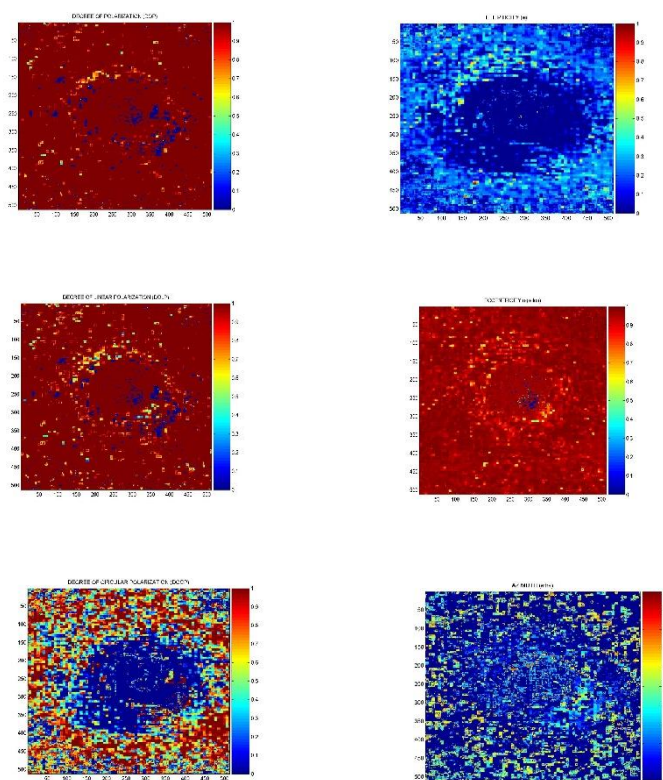


Fig.5. Images of DoP, DoLP and DoCP, Ellipticity, Eccentricity and fast axis orientation azimuth images of sample

After obtaining the values of the Stokes vector from the pictures, the parameters DoP, DoLP, and DoCP, as well as ellipticity, eccentricity & fast axis orientation azimuth, are computed with the help of Equations 21-26. Table 5.4 displays, for the sample of *Zingiber officinale*, the values that correspond to the sample's respective mean.

DoP	DoLP	DoCP	Ellipticity	Eccentricity	Azimuth
0.89405	0.837021	0.3142	0.171038	0.985264469	0.561509

Table 5.4: The average values of DOP, DOLP, and DOCP, as well as ellipticity and eccentricity and fast axis orientation Azimuth images of *Zingiber officinale*

To analyse the data from these tests, which was captured in the form of photographs, we carried out the steps outlined below. It was decided to crop the collected photos to the size of the light source (100 X 100 pixels). Pixel values for diattenuation, depolarization, and retardance were extracted from these photos after they were cropped. As a whole, these parameters' values were shown as an average across all pixels. In addition, we computed and compared Mueller images. The photos were scaled according to the Mueller matrix's first element (M11). For the purpose of making comparisons between multiple samples and distinguishing between them, Relevant

data were displayed after the decomposition graphs were normalized across columns. The Mueller pictures were processed in a similar fashion. The Degree of polarisation, Ellipticity, Eccentricity, and fast axis orientation azimuth were determined using the estimated stokes parameters. With the help of our experimental methods, we were able to collect the wood sample's optical signature with in format of the Mueller matrix.. The results show that the wood sample has polarisation anisotropic feature, as expected.

References:

- [1]. M. Losurdo, M. Bergmair, G. Bruno, D. Cattelan, C. Cobet, A. de Martino, K. Fleischer, Z. Dohcevic-Mitrovic, N. Esser, M. Galliet, R. Gajic, D. Hemzal, K. Hingerl, J. Humlicek, R. Ossikovski, Z. V. Popovic, and O. Saxl, "Spectroscopic ellipsometry and polarimetry for materials and systems analysis at the nanometer scale: state-of-the-art, potential, and perspectives," *J. Nanopart. Res.*, 1–34 (2009).
- [2]. R. A. Chipman, "Polarimetry," in *Handbook of Optics*, M. Bass, E. W. V. Stryland, D. R. Williams, and W. L. Wolfe, eds. (McGraw Hill, Inc., New York, 1995), Chap. 22.
- [3]. D. H. Goldstein, "Mueller matrix dual-rotating retarder polarimeter," *Appl. Opt.* 31(31), 6676–6683 (1992).
- [4]. R. A. Synowicki, J. N. Hilfiker, and P. K. Whitman, "Mueller matrix ellipsometry study of uniaxial deuterated potassium dihydrogen phosphate (DKDP)," *Thin Solid Films* 455–456, 624–627 (2004).
- [5]. J. N. Hilfiker, B. Johs, C. M. Herzinger, J. F. Elman, E. Montbach, D. Bryant, and P. J. Bos, "Generalized spectroscopic ellipsometry and Mueller-matrix study of twisted nematic and super twisted nematic liquid crystals," *Thin Solid Films* 455–456, 596–600 (2004).
- [6]. G. E. Jellison, and F. A. Modine, "Two-modulator generalized ellipsometry: theory," *Appl. Opt.* 36(31), 8190– 8198 (1997).
- [7]. C. Chen, M. W. Horn, S. Pursel, C. Ross, and R. W. Collins, "The ultimate in real-time ellipsometry: Multichannel Mueller matrix spectroscopy," *Appl. Surf. Sci.* 253(1), 38–46 (2006). 15. A. De Martino, Y. K. Kim, E. Garcia-Caurel, B. Laude, and B. Dré villon, "Optimized Mueller polarimeter with liquid crystals," *Opt. Lett.* 28(8), 616–618 (2003).
- [8]. S. Ben Hatit, M. Foldyna, A. De Martino, and B. Dré villon, "Angle-resolved Mueller polarimeter using a microscope objective," *Phys. Status Solidi A* 205(4), 743–747 (2008).
- [9]. P. S. Hauge, "Recent developments in instrumentation in ellipsometry," *Surf. Sci.* 96(1-3), 108–140 (1980).
- [10]. C. Chen, I. An, G. M. Ferreira, N. J. Podraza, J. A. Zapien, and R. W. Collins, "Multichannel Mueller matrix ellipsometer based on the dual rotating compensator principle," *Thin Solid Films* 455–456, 14–23 (2004).

- [11]. A. De Martino, E. Garcia-Caurel, B. Laude, and B. Drevillon, "General methods for optimized design and calibration of Mueller polarimeters," *Thin Solid Films* 455–456, 112–119 (2004).
- [12]. G. E. Jellison, Jr., "Spectroscopic ellipsometry data analysis: measured versus calculated quantities," *Thin Solid Films* 313–314(1-2), 33–39 (1998).
- [13]. A. Laskarakis, S. Logothetidis, E. Pavlopoulou, and A. Gioti, "Mueller matrix spectroscopic ellipsometry: formulation and application," *Thin Solid Films* 455–456, 43–49 (2004).
- [14]. Y. Zhang, and E. Bahar, *IEEE Trans. Antennas Propagat.* 47, 6 (1999).
- [15]. P. A. Letnes, A. A. Maradudin, T. Nordam, and I. Simonsen, *Phys. Rev. A* 86, 5 (2012)
- [16]. S. M. F. Nee, *Appl. Opt.* 40, 6 (2001).
- [17]. J. S. Tyo, D. L. Goldstein, D. B. Chenault, and J. A. Shaw, "Review of passive imaging polarimetry for remote sensing applications," *Appl. Opt.* 45, 5453–5469 (2006).
- [18]. V. V. Tuchin, L. Wang, and D. A. Zimnyakov, *Optical Polarization in Biomedical Applications* (Springer, 2006).
- [19]. N. Ghosh and I. A. Vitkin, "Tissue polarimetry: concepts, challenges, applications, and outlook," *J. Biomed. Opt.* 16, 110801 (2011).
- [20]. P. S. Hauge, "Recent developments in instrumentation in ellipsometry," *Surf. Sci.* 96, 108–140 (1980).
- [21]. R. A. Chipman, "Mueller matrices," in *Handbook of Optics*, M. Bass and V. N. Mahajan, eds. (McGraw-Hill, 2010), Vol. I, Chaps. 14 and 15.
- [22]. C. Brosseau, *Fundamentals of Polarized Light* (Wiley, 1998).